

RESEARCH ARTICLE

A role for Gic1 and Gic2 in Cdc42 polarization at elevated temperature

Christine N. Daniels, Trevin R. Zyla, Daniel J. Lew *

Department of Pharmacology and Cancer Biology, Duke University, Durham, North Carolina, United States of America

* daniel.lew@duke.edu



Abstract

The conserved Rho-family GTPase Cdc42 is a master regulator of polarity establishment in many cell types. Cdc42 becomes activated and concentrated in a region of the cell cortex, and recruits a variety of effector proteins to that site. In turn, many effectors participate in regulation of cytoskeletal elements in order to remodel the cytoskeleton in a polarized manner. The budding yeast *Saccharomyces cerevisiae* has served as a tractable model system for studies of cell polarity. In yeast cells, Cdc42 polarization involves a positive feedback loop in which effectors called p21-activated kinases (PAKs) act to recruit a Cdc42-directed guanine nucleotide exchange factor (GEF), generating more GTP-Cdc42 in areas that already have GTP-Cdc42. The GTPase-interacting components (GICs) Gic1 and Gic2 are also Cdc42 effectors, and have been implicated in regulation of the actin and septin cytoskeleton. However, we report that cells lacking GICs are primarily defective in polarizing Cdc42 itself, suggesting that they act upstream as well as downstream of Cdc42 in yeast. Our findings suggest that feedback pathways involving GTPase effectors may be more prevalent than had been appreciated.

OPEN ACCESS

Citation: Daniels CN, Zyla TR, Lew DJ (2018) A role for Gic1 and Gic2 in Cdc42 polarization at elevated temperature. PLoS ONE 13(12): e0200863. <https://doi.org/10.1371/journal.pone.0200863>

Editor: Robert Alan Arkowitz, Institute of Biology Valrose, FRANCE

Received: June 28, 2018

Accepted: November 9, 2018

Published: December 19, 2018

Copyright: © 2018 Daniels et al. This is an open access article distributed under the terms of the [Creative Commons Attribution License](https://creativecommons.org/licenses/by/4.0/), which permits unrestricted use, distribution, and reproduction in any medium, provided the original author and source are credited.

Data Availability Statement: All relevant data are within the paper and its Supporting Information files.

Funding: This study was funded by the National Institute of General Medical Sciences, via grants GM62300 and GM122488 to Daniel Lew. The funders had no role in study design, data collection and analysis, decision to publish, or preparation of the manuscript.

Competing interests: The authors have declared that no competing interests exist.

Introduction

Regulation of cell shape is central to cell proliferation as well as many aspects of cell function. Cell shape is in large part governed by the cytoskeleton, which itself is regulated by multiple signaling pathways. Among the most prominent and widespread cytoskeleton-regulating pathways are those mediated by evolutionarily conserved small GTPases of the Rho family, including Rho, Rac, and Cdc42 [1]. These GTPases are thought to act as molecular switches, toggling between an inactive GDP-bound state and an active GTP-bound state. Intrinsic rates of activation (GDP/GTP exchange) and inactivation (GTP hydrolysis) are slow, and can be greatly enhanced by guanine nucleotide exchange factors (GEFs) and GTPase activating proteins (GAPs), respectively [2]. Rho-family GTPases are prenylated and reside primarily on the cytoplasmic leaflet of cellular membranes, although they can be extracted to the cytoplasm by guanine nucleotide dissociation inhibitors (GDIs) [3, 4]. Signaling pathways controlling cell shape often act by regulating and localizing the activities of GEFs and GAPs, leading to specific spatiotemporal patterns of GTPase activity.

Information encoded by the abundance and spatial pattern of GTPase activity is decoded by a set of GTPase-specific “effectors”, which are proteins that bind to the active but not the inactive form of the GTPase. Most known effectors are cytoplasmic proteins whose activity and localization within the cell can change as a result of GTPase binding. Effector localization and activity can also be regulated by other signals (e.g. phosphoinositides), allowing for complex combinatorial control of the cytoskeleton. Among the most intensively studied effectors are the p21-activated kinases (PAKs) [5], the WASP and WAVE regulators of branched actin nucleation by Arp2/3 complexes [6], and the formins that nucleate and accelerate polymerization of unbranched actin filaments [7]. In aggregate, GTPase signaling via effectors is responsible for sculpting the cytoskeleton, in addition to other functions.

One major role for Cdc42 and Rac concerns the establishment of cell polarity [8]. Studies of polarity establishment in the model yeast *Saccharomyces cerevisiae* led to the identification of both positive feedback and negative feedback loops built into the polarity circuit [9, 10]. In the positive feedback loop, effector PAKs are recruited to bind GTP-Cdc42, and they bind a scaffold protein called Bem1, which in turn binds to Cdc24, the yeast GEF for Cdc42 [11]. These interactions mean that wherever there is a slight local accumulation of GTP-Cdc42, recruitment of PAK-Bem1-Cdc24 will lead to enhanced GEF activity, leading to further local Cdc42 activation in a positive feedback loop [12]. Once GTP-Cdc42, PAKs, and Cdc24 co-accumulate to high levels due to positive feedback, the active PAKs promote multi-site phosphorylation of Cdc24 [13–15]. This phosphorylation reduces GEF activity [16], possibly by more than one mechanism [17], yielding a negative feedback loop. Thus, in addition to signaling to the cytoskeleton downstream of the GTPase, some effectors can also act as feedback transducers to regulate the local activation of the GTPase itself.

Analysis of several Cdc42 and Rac effectors, including the PAKs, led to the identification of a conserved Cdc42/Rac interactive binding (CRIB) motif that recognizes GTP-Cdc42 and GTP-Rac [18]. Bioinformatic searches for other CRIB-containing proteins identified the GTPase interacting components (GICs), Gic1 and Gic2, in *S. cerevisiae* [19, 20]. GICs are small proteins that encode membrane-binding amphipathic helices [21] and a short conserved GIC motif of unknown function [22] in addition to the CRIB domain. The mammalian binder of Rho GTPase (BORG) proteins have a similar organization and may be homologs of the GICs [23]. In yeast cells, GICs are concentrated at polarity sites marked by active Cdc42 [19, 20]. Deletion of either *GIC1* or *GIC2* does not produce a dramatic phenotype, but cells lacking both GICs are large and misshapen, and (in haploids) fail to proliferate at high temperature (37°C) [19, 20].

Subsequent work implicated GICs in regulating both the actin and septin cytoskeletons. In yeast cells, filamentous actin is present in actin cables (linear filament bundles oriented towards the polarity site that enable type V myosin-mediated cargo delivery to the bud) and in cortical actin patches (branched actin structures that promote invagination of the plasma membrane at sites of endocytosis) [24, 25]. In polarized cells, actin patches accumulate near the polarity site and cables are oriented towards that site. However, in *gic1Δ gic2Δ* haploids at 37°C, most cells display randomly distributed actin patches, and fail to form a bud [20]. Moreover, Gic2 interacts with and helps to localize the formin Bni1 to the polarity site, providing a potential mechanism for actin regulation [26].

Septins are conserved filament-forming proteins that assemble into a ring surrounding the polarity site following polarity establishment in yeast [27, 28]. However, in *gic1Δ gic2Δ* haploids at 37°C, most cells fail to recruit septins to the polarity site [29]. GICs were shown to bind septins and affect interactions between septin polymers in vitro, providing a potential mechanism for septin regulation [29, 30].

In addition to the studies implicating GICs as mediators of Cdc42-induced actin and septin rearrangements, a genetic interaction was identified between GICs and the Ras-family GTPase Rsr1 [31]. Rsr1 mediates communication between various transmembrane “landmark” proteins, which mark preferred sites for subsequent polarization, and the Cdc42-based polarity establishment pathway [32]. Unlike *gic1Δ gic2Δ* or *rsr1Δ* mutants, which are viable at 24°C, *gic1Δ gic2Δ rsr1Δ* triple mutants were lethal. This suggested that GICs might act upstream of Cdc42, in parallel with Rsr1, as well as downstream of Cdc42.

Here, we have investigated the *gic1Δ gic2Δ* phenotype in greater detail, using live-cell imaging of cells bearing probes for polarity regulators Cdc42 and Bem1. We found that at 37°C, a majority of *gic1Δ gic2Δ* cells failed to polarize at all. This finding provides an alternative interpretation for previous findings in which the mutants failed to polarize actin or septins: these defects could be secondary effects stemming from a more fundamental lack of Cdc42 polarization. A subset of the *gic1Δ gic2Δ* mutant cells did polarize Cdc42 and Bem1 at 37°C, and those cells did not display any obvious difficulty in forming a bud, suggesting that downstream cytoskeletal defects (if present) were quite mild. We conclude that, as suggested by Kawasaki et al. [31], a major role of the GICs is to promote and/or maintain Cdc42 polarization.

Results

Polarity establishment in yeast is regulated by the cell cycle. In particular, activation of G1 cyclin-dependent kinase (CDK) complexes at a commitment point called start in G1 promotes Cdc42 polarization [13]. G1 CDK activation at start occurs through a transcriptional positive feedback loop in which rising CDK activity promotes the inactivation and nuclear export of the repressor Whi5, allowing more transcription of G1 cyclins [33–35]. Commitment to enter the cell cycle (i.e. start) occurs when 50% of nuclear Whi5 has been exported, at which point the positive feedback loop becomes self-sustaining [36]. We used Whi5-GFP or Whi5-tdTomato as a probe for start, and Bem1-tdTomato [9] or GFP-Cdc42 [16] as a probe for polarization. Haploid cells were grown at 24°C and arrested in G1 by treatment with mating pheromone. Arrested cells were released to proceed into the cell cycle by washing out the pheromone, and placed on microscope slabs at 37°C. Live cell imaging by confocal fluorescence microscopy was then employed to monitor probe localization.

In wild-type cells under these conditions, Whi5 nuclear export was closely followed by Bem1 (Fig 1 and S1 Movie) or Cdc42 (Fig 1 and S2 Movie) polarization. However, in *gic1Δ gic2Δ* cells there was a heterogeneous phenotype: a majority of cells failed to polarize either Bem1 (Fig 1B and S1 Movie) or Cdc42 (Fig 1C and S2 Movie) after Whi5 nuclear exit. A substantial minority of cells did polarize the probes, although polarity establishment occurred somewhat later than in wild-type cells. Quantification revealed that 30%-40% of *gic1Δ gic2Δ* cells were able to form buds, but compared to wild-type cells the start-to-budding interval was longer (Fig 2A). Similarly, 30%-40% of *gic1Δ gic2Δ* cells were able to polarize Bem1 or Cdc42 (Fig 2B), but with a longer interval between start and polarization (Fig 2C: median 7.5 min for wild-type and 13.5 min for *gic1Δ gic2Δ*, $p < 0.01$ by Mood's median test). For the subset of *gic1Δ gic2Δ* cells that did polarize, the interval between polarization and budding was similar to that in wild-type cells (Fig 2D). Thus, the major defect exhibited by *gic1Δ gic2Δ* cells at 37°C was an inability to establish and/or maintain polarity.

Polarity establishment requires activation of Cdc42, which is promoted by the GEF Cdc24 and antagonized by the GAPs Bem2, Bem3, Rga1, and Rga2 [32]. Thus, possible bases for the defect in polarity establishment in *gic1Δ gic2Δ* cells include that they have insufficient GEF, Cdc42, or Bem1, or excess GAPs. As an initial attempt to test that hypothesis, we compared the abundance of these regulators in wild-type and *gic1Δ gic2Δ* cells. We noted no significant

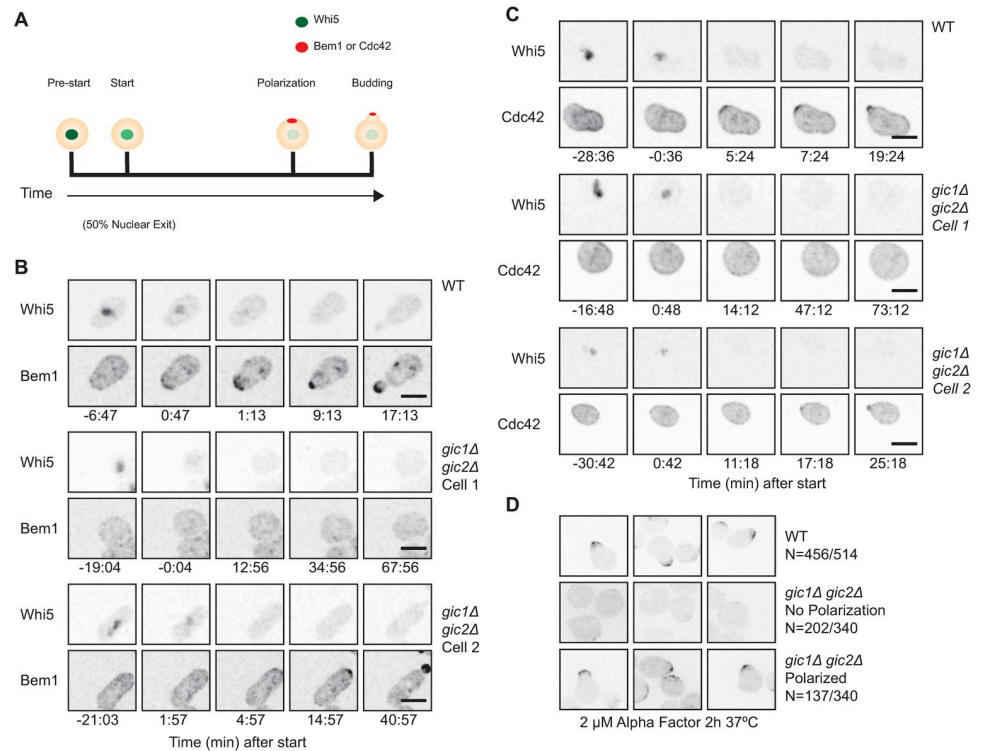


Fig 1. Delayed or blocked polarity establishment in *gic1Δ gic2Δ* mutants at 37°C. (A) Schematic depicting Whi5 and polarity protein distributions as cells proceed through the cell cycle. In early G1 phase (pre-start), Whi5 is concentrated in the nucleus (green) and polarity factors are dispersed. As CDK activation occurs, Whi5 is exported from the nucleus (when 50% of Whi5 has been exported the cells commit to enter the cell cycle at “start”). CDK activation triggers localization of polarity factors to a cortical site (red: polarization) from which the bud later emerges (bud). (B) Inverted maximum projection montages of selected timepoints for representative cells from movies of wild-type (WT: DLY19654) or mutant (*gic1Δ gic2Δ*: DLY20961) cells progressing through the cell cycle at 37°C. The cells express Whi5-GFP (top row) and Bem1-tdTomato (bottom row) probes. Cells were synchronized in G1 by pheromone arrest-release, and time relative to start is indicated. Wild-type cells polarized shortly after start, whereas 58% of *gic1Δ gic2Δ* cells failed to polarize (cell 1); the others polarized, often after a delay (cell 2). (C) Display as for (B) but with strains expressing Whi5-tdTomato (top row) and GFP-Cdc42 (bottom row). Wild type: DLY21726. *gic1Δ gic2Δ*: DLY21728. Wild-type cells polarized shortly after start, whereas 76% of *gic1Δ gic2Δ* cells failed to polarize (cell 1); the others polarized, often after a delay (cell 2). (D) Wild-type (WT: DLY19654) and mutant (*gic1Δ gic2Δ*: DLY20961) cells were grown at 24°C, placed on a slab containing 2 μM α-factor, and incubated at 37°C for 2 h. Cells that arrested in G1 (scored by the presence of nuclear Whi5) were examined for polarization of Bem1. Inverted maximum projection montages of selected cells are shown: wild-type cells polarized, whereas 60% of *gic1Δ gic2Δ* cells failed to polarize (middle row); the others polarized (bottom row). Scale bar, 5 μm.

<https://doi.org/10.1371/journal.pone.0200863.g001>

differences, either when the cells were grown at 24°C (Fig 3A) or 37°C (Fig 3B). Many of the regulators undergo phosphorylation, which is thought to regulate their activity [13–16, 37, 38]. Although we detected altered-mobility species in many of the blots, we did not find any systematic difference between wild-type and *gic1Δ gic2Δ* cells.

We next attempted a genetic approach to test whether mutations in regulators might enhance or suppress the phenotype of *gic1Δ gic2Δ* cells. Although *gic1Δ gic2Δ* mutants are lethal at 37°C following tetrad dissection (Fig 4A), growth of *gic1Δ gic2Δ* mutants at 24°C led to a rapid accumulation of spontaneous suppressors, such that subsequent transfer to 37°C was not uniformly lethal. This high frequency of suppression made it impossible to reliably test whether mutations in regulators were able to suppress the phenotype. We speculated that because a subpopulation of mutant cells was able to bud (Figs 1 and 2), strong selection pressure could be applied to the expanding population, yielding a high spontaneous suppression

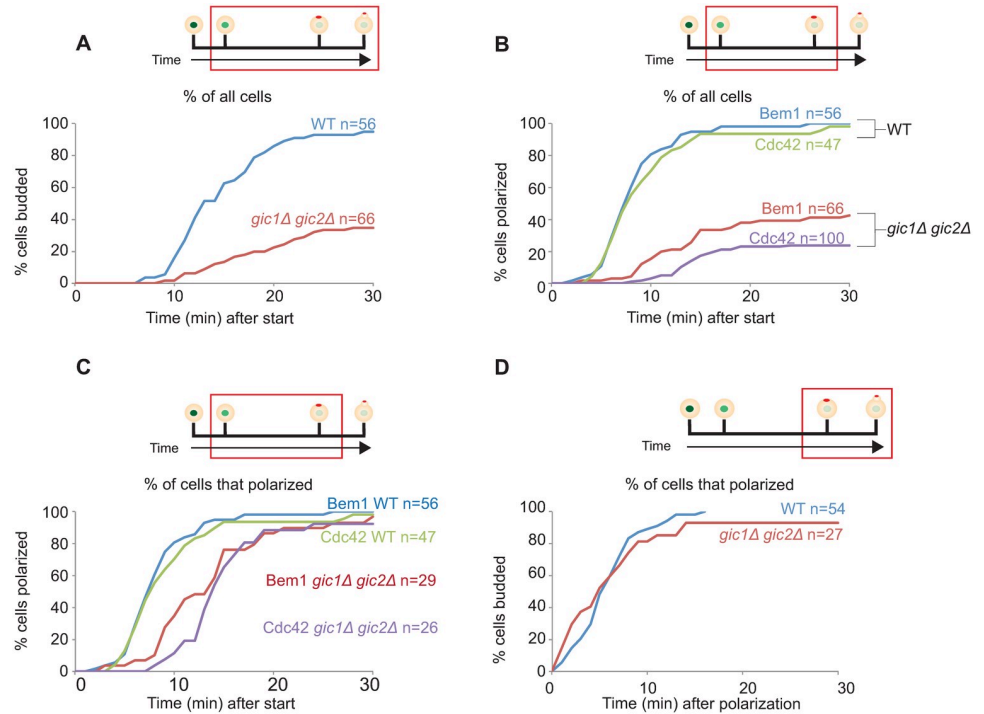


Fig 2. Quantification of polarity establishment in *gic1Δ gic2Δ* mutants at 37°C. Time intervals between start and bud emergence (A), and between start and polarization (B), were scored from the time-lapse movies described in Fig 1. Top: schematics as in Fig 1A, indicating the interval scored (red box). Bottom: graphs showing the cumulative % of cells (y axis) that completed the interval by the indicated time (x axis). The number of cells scored for each plot is indicated (n). Intervals between start and polarization (C), and between polarization and bud emergence (D) are also plotted including only the subset of cells that polarized (hence the lower n), allowing comparison of timing. (A–D) plot data for strains expressing Bem1-tdTomato (as in Fig 1B), while (B) additionally plots data for strains expressing GFP-Cdc42 (as in Fig 1C).

<https://doi.org/10.1371/journal.pone.0200863.g002>

frequency. Such suppression might occur at many loci or just a few, and we reasoned that in the latter case, identification of the basis for spontaneous suppression might be informative with regard to the specific molecular defect that prevents polarization of a majority of *gic1Δ gic2Δ* cells.

We picked 10 independent unsuppressed haploid *gic1Δ gic2Δ* colonies growing at 24°C, and spread a million cells of each colony on a rich media plate that was incubated at 37°C. Multiple colonies arose spontaneously on each plate, ranging from large to tiny in size (Fig 4B). We picked a large colony from each plate, and mated them to an unsuppressed *gic1Δ gic2Δ* of the opposite mating type. Upon sporulation of the resulting diploids, viability at 37°C segregated 2:2 in tetrads in 9 cases, showing that suppression was due to a single Mendelian locus in these independently derived strains (Fig 4B and Table 1).

To assess whether the independent suppressors occurred at the same or different loci, we performed pairwise crosses between *gic1Δ gic2Δ* mutants carrying the different suppressors. In all cases, diploids generated by crossing one suppressed strain to another showed 4:0 segregation for viability at 37°C (Fig 4B). This indicates that all suppressors are tightly linked, and likely to be in the same locus.

To characterize the suppressed phenotype, we performed live cell imaging of suppressed strains carrying Whi5-GFP and Bem1-tdTomato. We found that suppressed strains were similar to wild-type in terms of the efficiency and timing of polarization relative to start (Fig 5). Thus, suppression is highly effective in restoring the ability to polarize.

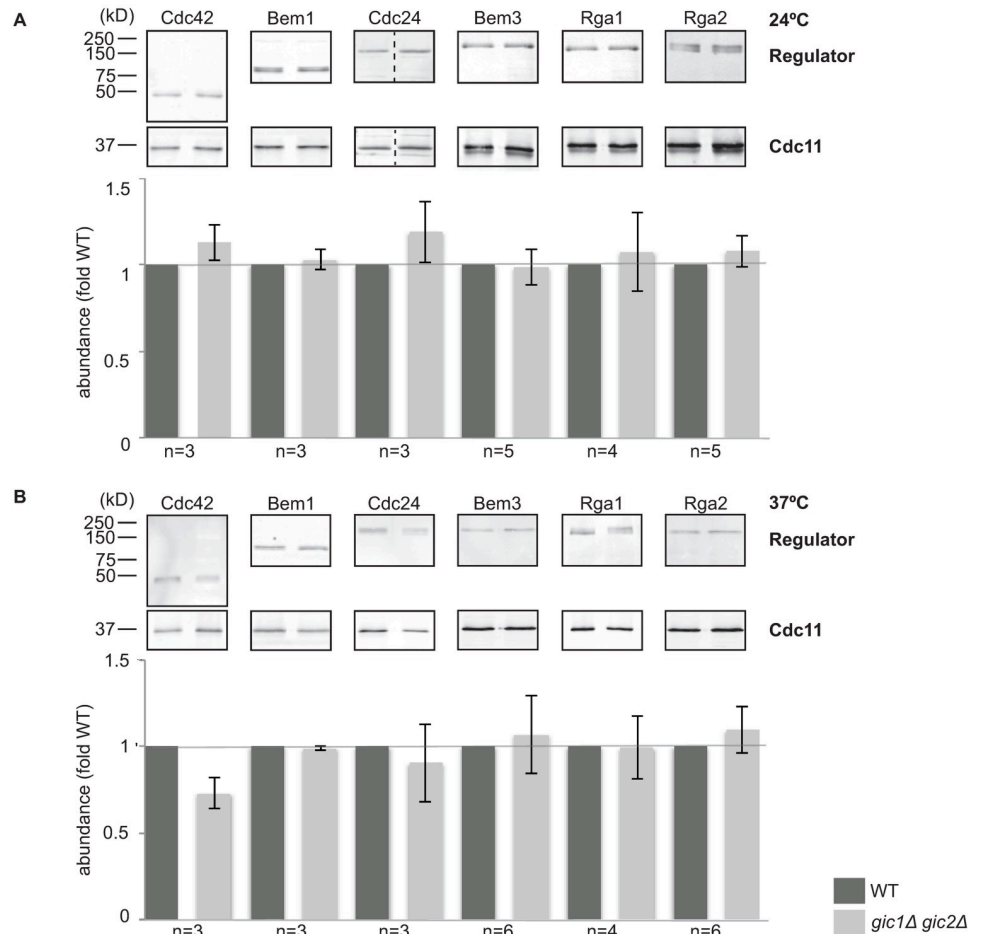


Fig 3. Abundance of Cdc42 and its regulators in *gic1Δ gic2Δ* mutants. (A) Anti-HA Western blot to compare the abundance of Cdc24-3HA expressed at the endogenous locus in wild-type (DLY15429) and *gic1Δ gic2Δ* (DLY21815) strains. Anti-GFP Western blots to compare abundance of Bem1-GFP (wild-type, DLY10005; *gic1Δ gic2Δ*, DLY20597) and GFP-Cdc42 (wild-type, DLY21726; *gic1Δ gic2Δ*, DLY21728). Anti-myc Western blots to compare abundance of Bem3-12myc (wild-type, DLY11483; *gic1Δ gic2Δ*, DLY22232), Rga1-12myc (wild-type, DLY21093; *gic1Δ gic2Δ*, DLY22235), and Rga2-12myc (wild-type, DLY11847; *gic1Δ gic2Δ*, DLY22232) expressed at the endogenous loci. Loading control is a blot of Cdc11 (a septin) in the same lysates. Cells were grown to mid-log phase and lysates were prepared as described in Methods. Quantification of each blot (fluorescence intensity of secondary antibody for each regulator normalized to its corresponding loading control) is shown in the bar graph below each blot. When independent Western blots were performed, the number of blots is indicated and the bar graphs show mean and standard error of the mean. (B) Western blots were repeated using lysates from cells that were shifted to 37°C for 6 h prior to lysate preparation. Dashed lines indicate instances in which the two lanes were not adjacent in the original gel and the intervening lanes have been removed for clarity.

<https://doi.org/10.1371/journal.pone.0200863.g003>

Discussion

Previous studies identified roles for Gic1 and Gic2 in regulating actin or septin organization downstream of Cdc42. As GICs are effectors that bind specifically to GTP-Cdc42, it was natural to expect roles of GICs acting downstream of Cdc42. However, the discovery of synthetic lethality between *rsr1Δ* and *gic1Δ gic2Δ* mutants [31] indicated that GICs might also act upstream of Cdc42. Our major finding is that GICs are required for efficient and timely polarization of Cdc42 at 37°C, strongly supporting the conclusion that GICs act upstream of Cdc42. Given the presence of both positive and negative feedback in the polarity circuit [10], such

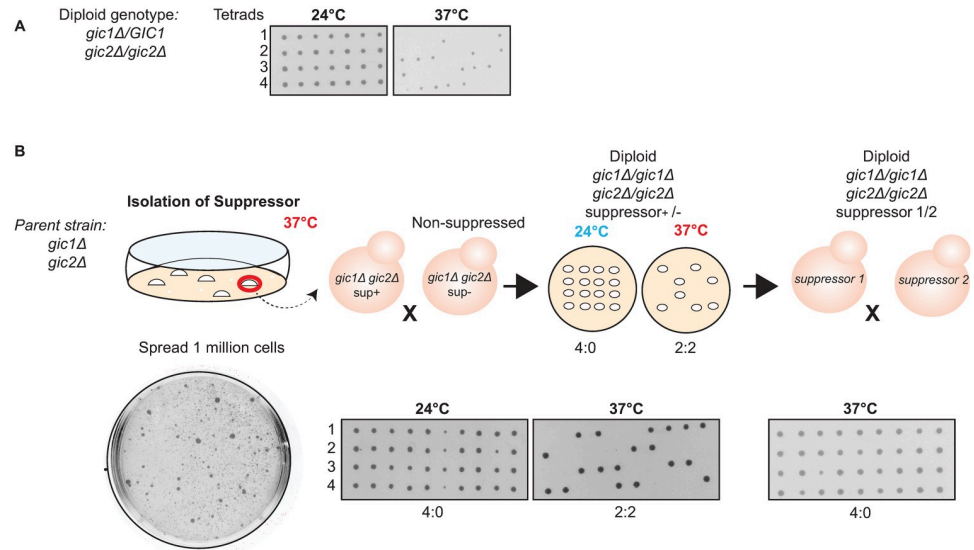


Fig 4. *gic1Δ gic2Δ* mutants spontaneously acquire a Mendelian suppressor mutation. (A) *gic1Δ gic2Δ* mutants are inviable at 37°C. A diploid strain with the indicated genotype (DLY21711) was sporulated and tetrads (four spores in a vertical column) were dissected onto plates that were incubated at the indicated temperature. Tetrads contain two *GIC1 gic2Δ* spores and two *gic1Δ gic2Δ* spores. At 24°C all four spores were viable and gave rise to colonies, but at 37°C two spores from each tetrad died. Replica plating confirmed that the dead spores were the *gic1Δ gic2Δ* cells. (B) Isolation and genetic characterization of spontaneous *gic1Δ gic2Δ* suppressors. Cells of a *gic1Δ gic2Δ* strain (DLY20961) were streaked for single colonies. One million cells from each colony were plated on rich media and incubated at 37°C for 3 days. Although most cells died, several heterogeneously sized colonies were able to grow (example plate, bottom left), and one large colony from each independent plate was picked for further analysis. Suppressed cells were mated to a non-suppressed *gic1Δ gic2Δ* strain of opposite mating type (DLY21941), and the resulting diploids were sporulated and dissected as in (A). Tetrads showed 2:2 viability (middle panels) at 37°C indicating segregation of the suppressor as a single Mendelian locus. Independent suppressed strains (from different initial colonies) were then mated to each other and the resulting diploids were sporulated and dissected as in (A). All tetrads showed 4:0 viability at 37°C (right panels) indicating that the suppressors all map to the same locus. Sequencing confirmed that suppressed strains retained the *gic1Δ* and *gic2Δ* mutations.

<https://doi.org/10.1371/journal.pone.0200863.g004>

upstream action may be indicative of role(s) for GICs in modulating feedback, as discussed below.

There are several potential explanations for these findings. First, GICs might play dual roles, acting both upstream of Cdc42 and downstream of Cdc42 in separate pathways. A preliminary examination of the levels of known Cdc42 regulators did not reveal any differences

Table 1. Tetrad analysis of diploids from crosses between suppressed and non-suppressed *gic1Δ gic2Δ* strains.

Suppressor	% of tetrads segregating 2:2 for viability at 37°C	Number of tetrads
1	100	22
2	96	25
3	92	26
4	78	18
5	100	25
6	78	18
7	100	24
8	89	19
9	95	21

<https://doi.org/10.1371/journal.pone.0200863.t001>

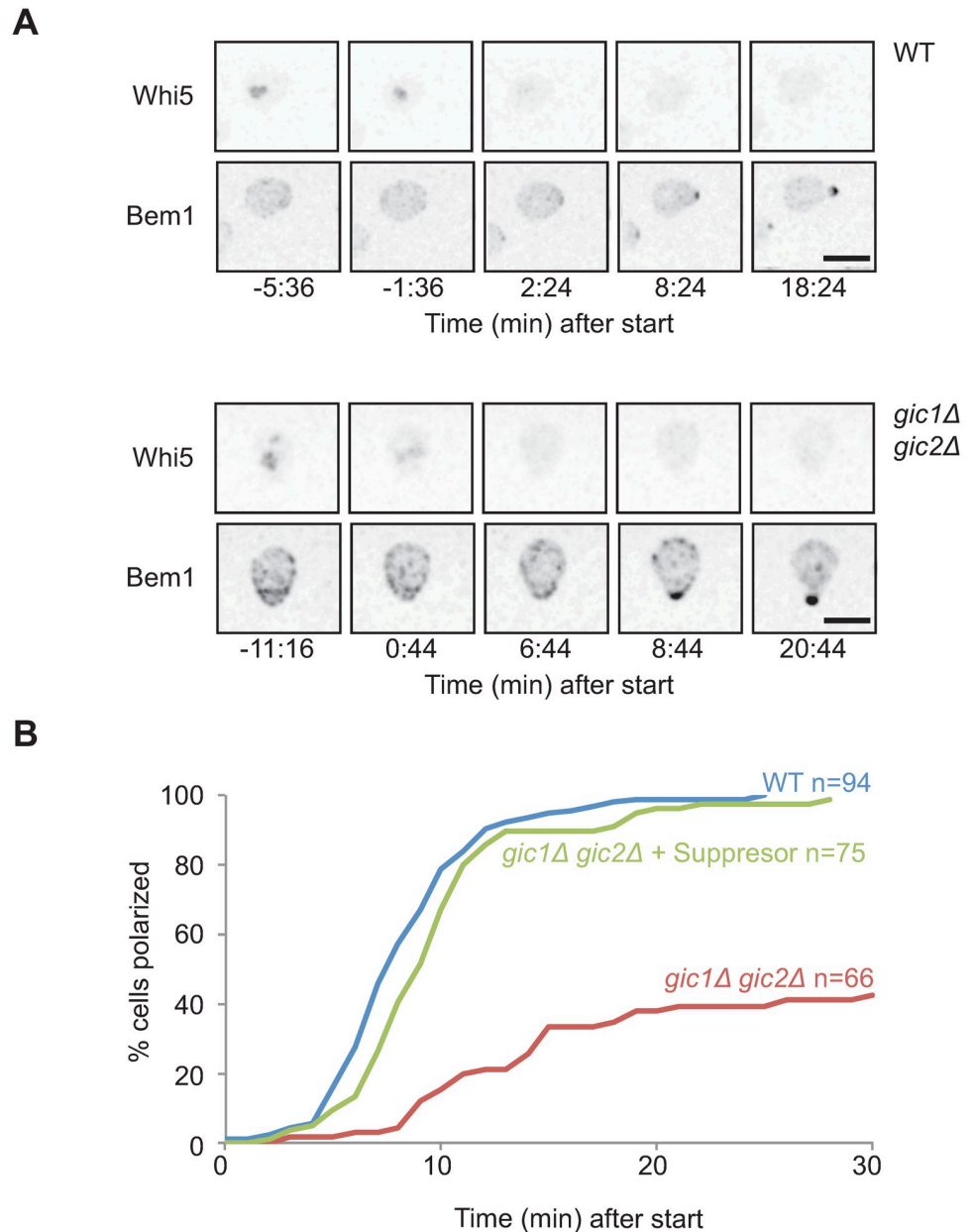


Fig 5. Suppressed *gic1Δ gic2Δ* mutants polarize like wild-type cells. (A) Inverted maximum projection montages of selected timepoints for representative cells from movies of wild-type (WT: DLY19654) or suppressed *gic1Δ gic2Δ* (DLY22968) cells progressing through the cell cycle at 37°C. The cells express Whi5-GFP (top row) and Bem1-tdTomato (bottom row) probes. Cells were synchronized in G1 by pheromone arrest-release, and time relative to start is indicated. Scale bar, 5 μm. (B) Time intervals between start and polarization were scored from the time-lapse movies above as in Fig 2B. The number of cells scored for each plot is indicated (n). Data for wild-type strain are from same conditions as in Fig 2B but different movies, taken contemporaneously with those for the suppressed strain. Data for unsuppressed *gic1Δ gic2Δ* cells is reproduced from Fig 2 to allow direct comparison to suppressed strain.

<https://doi.org/10.1371/journal.pone.0200863.g005>

between wild-type and *gic1Δ gic2Δ* mutant cells, but it remains possible that GICs affect the activity rather than the abundance of these regulators.

Second, GICs may simply act as downstream effectors of Cdc42, mediating cytoskeletal reorganization. Because Cdc42 is known to polarize even in the absence of F-actin [39, 40] or

Table 2. Yeast strains used in this study.

Strain	Genotype	Notes
DLY10001	<i>MATa/α ABP1-mCherry:Kan/ABP1 Bem1-GFP::LEU2/BEM1 rsr1::TRP1/RSR1</i>	
DLY10005	<i>MATa ABP1-mCherry:Kan Bem1-GFP::LEU2</i>	Derived by dissection of tetrads from DLY10001
DLY11843	<i>MATα BEM3-12myc:URA3</i>	
DLY11847	<i>MATα RGA2-12myc:URA3</i>	
DLY15073	<i>MATa/α CDC24-3HA:kan^R/CDC24</i>	
DLY15429	<i>MATa CDC24-3HA:kan^R</i>	Derived by dissection of tetrads from DLY15073
DLY19652	<i>MATa/α BEM1-tdTomato:HIS3/BEM1 WHI5-GFP:HIS3/WHI5 rsr1::TRP1/RSR1</i>	
DLY19654	<i>MATa BEM1-tdTomato:HIS3 WHI5-GFP:HIS3</i>	Derived by dissection of tetrads from DLY19652
DLY20597	<i>MATa BEM1-GFP:LEU2 ABP1-mCherry:Kan gic1::TRP1 gic2::HIS3</i>	
DLY20961	<i>MATa BEM1-tdTomato:HIS3 WHI5-GFP:HIS3 gic1::TRP1 gic2::HIS3</i>	Derived by dissection of tetrads from DLY20962
DLY20962	<i>MATa/α BEM1-tdTomato:HIS3/BEM1 WHI5-GFP:HIS3/WHI5 gic1::TRP1/GIC1 gic2::HIS3/GIC2</i>	
DLY21092	<i>MATa/α RGA1-12myc:URA3/RGA1</i>	
DLY21093	<i>MATα RGA1-12myc:URA3</i>	Derived by dissection of tetrads from DLY21092
DLY21445	<i>MATa/α WHI5-tdTomato:URA3/WHI5 GFP-linker-CDC42:URA3/CDC42 gic1::TRP1/GIC1 gic2::HIS3/GIC2</i>	
DLY21711	<i>MATa/α gic1::TRP1/gic1::TRP1 gic2::HIS3/GIC2</i>	
DLY21726	<i>MATa WHI5-tdTomato:URA3 GFP-linker-CDC42:URA3</i>	Derived by dissection of tetrads from DLY21445
DLY21728	<i>MATa WHI5-tdTomato:URA3 GFP-linker-CDC42:URA3 gic1::TRP1 gic2::HIS3</i>	Derived by dissection of tetrads from DLY21445
DLY21811	<i>MATa/α gic1::TRP1/GIC1 gic2::HIS3/GIC2 CDC24-3HA:kan^R/CDC24</i>	
DLY21814	<i>MATa gic1::TRP1 gic2::HIS3 CDC24-3HA:kan^R</i>	Derived by dissection of tetrads from DLY21811
DLY22230	<i>MATa/α gic1::TRP1/GIC1 gic2::HIS3/GIC2 BEM3-12myc:URA3/BEM3</i>	
DLY22232	<i>MATα gic1::TRP1 gic2::HIS3 BEM3-12myc:URA3</i>	Derived by dissection of tetrads from DLY22230
DLY22233	<i>MATa/α gic1::TRP1/GIC1 gic2::HIS3/GIC2 RGA1-12myc:URA3/RGA1</i>	
DLY22235	<i>MATα gic1::TRP1 gic2::HIS3 RGA1-12myc:URA3</i>	Derived by dissection of tetrads from DLY22233
DLY22236	<i>MATa/α gic1::TRP1/GIC1 gic2::HIS3/GIC2 RGA2-12myc:URA3/RGA2</i>	
DLY22238	<i>MATα gic1::TRP1 gic2::HIS3 RGA2-12myc:URA3</i>	Derived by dissection of tetrads from DLY22236
DLY22968	<i>MATa BEM1-tdTomato:HIS3 WHI5-GFP:HIS3 gic1::TRP1 gic2::HIS3 Suppressor1</i>	Parent strain DLY20961
DLY22969	<i>MATa BEM1-tdTomato:HIS3 WHI5-GFP:HIS3 gic1::TRP1 gic2::HIS3 Suppressor2</i>	Parent strain DLY20961
DLY22970	<i>MATa BEM1-tdTomato:HIS3 WHI5-GFP:HIS3 gic1::TRP1 gic2::HIS3 Suppressor3</i>	Parent strain DLY20961
DLY22971	<i>MATa BEM1-tdTomato:HIS3 WHI5-GFP:HIS3 gic1::TRP1 gic2::HIS3 Suppressor4</i>	Parent strain DLY20961

(Continued)

Table 2. (Continued)

Strain	Genotype	Notes
DLY22972	<i>MATa BEM1-tdTomato:HIS3 WHI5-GFP:HIS3 gic1::TRP1 gic2::HIS3 Suppressor5</i>	Parent strain DLY20961
DLY22973	<i>MATa BEM1-tdTomato:HIS3 WHI5-GFP:HIS3 gic1::TRP1 gic2::HIS3 Suppressor6</i>	Parent strain DLY20961
DLY22974	<i>MATa BEM1-tdTomato:HIS3 WHI5-GFP:HIS3 gic1::TRP1 gic2::HIS3 Suppressor7</i>	Parent strain DLY20961
DLY22975	<i>MATa BEM1-tdTomato:HIS3 WHI5-GFP:HIS3 gic1::TRP1 gic2::HIS3 Suppressor8</i>	Parent strain DLY20961
DLY22976	<i>MATa BEM1-tdTomato:HIS3 WHI5-GFP:HIS3 gic1::TRP1 gic2::HIS3 Suppressor9</i>	Parent strain DLY20961

<https://doi.org/10.1371/journal.pone.0200863.t002>

polymerized septins [41], this alone would not necessarily yield the observed defects in Cdc42 polarization. However, it could be that the particular cytoskeletal misregulation that occurs in *gic1Δ gic2Δ* mutants triggers a stress response that blocks effective Cdc42 polarization. Although stress pathways can act to block polarization [42, 43], we believe this scenario is unlikely.

Third, and perhaps most likely, GICs could operate as part of a positive feedback loop in which GTP-Cdc42 acts to promote further local accumulation of GTP-Cdc42. This would explain why cells lacking GICs have difficulties in polarizing Cdc42, and there is precedent for such feedback in the role of PAKs and Bem1 [10, 11]. In addition, one could imagine that GICs modulate the negative feedback loop in which PAK-mediated GEF phosphorylation reduces GEF activity [16], and that in the absence of GICs this inhibitory pathway is too powerful. However, the mechanism by which GICs might function in either positive or negative feedback remains mysterious.

Cells growing at 24°C do not require GICs for successful proliferation, suggesting that there are parallel pathways that can operate in the absence of GICs. Alternatively, it could be that GIC pathways are only engaged in order to deal with thermal stress. The growth defect of haploid cells lacking GICs can be suppressed by overexpression of Cdc42 [20], and diploid cells lacking GICs are able to proliferate successfully even at 37°C [44]. Other mutants (e.g. lacking the formin Bni1) display more severe phenotypes in diploids than in haploids [44]. The basis for these differences is unclear. We found that in our strain background, *gic1Δ gic2Δ* mutants frequently acquired spontaneous suppressors, and a genetic analysis indicated that several independently isolated suppressors all mapped to the same locus. Identification of the suppressor gene may provide insight into the role of GICs in promoting Cdc42 polarization.

While this paper was in revision, an independent study on GICs was published that reached similar conclusions to ours based on parallel experiments [45].

Materials and methods

Yeast strains and growth conditions

The yeast strains used in this study are in the YEF473 strain background (*his3-Δ200 leu2-Δ1 lys2-801 trp1-Δ63 ura3-52*) [46] and are listed in Table 2. Standard yeast molecular and genetic manipulations were used to construct strains, with additional precautions due to the high propensity of strains lacking GICs to become genetically suppressed. *GIC1* and *GIC2* deletions were generated by the one-step PCR-based method [47] with pRS304 as template for *gic1::TRP1* and pRS403 as template for *gic2::HIS3*.

Deletions were introduced into diploid strains, and diploids containing at least one wild-type GIC gene were used as strain construction intermediates to avoid selection for suppressors. In cases where strain construction involved a haploid *gic1::TRP1 gic2::HIS3* intermediate, we introduced a *URA3*-marked 2 μ m plasmid (pDLB2693) carrying wild-type *GIC2* into the parent diploid strain and maintained the plasmid in the derived haploid so as to avoid selecting for suppressors. Loss of the plasmid was induced when needed by growth on plates containing 5-fluoroorotic acid (5-FOA) [48].

Gene tagging at endogenous loci was previously described for Whi5-GFP [36], Whi5-tdTomato [49], Bem1-tdTomato [9] and Bem2-12myc [50]. The GFP-linker-Cdc42 probe was expressed in addition to endogenous untagged CDC42 (as the GFP-tagged version is not fully functional on its own) as described [16].

The Cdc24-3HA allele was generated by the PCR-based gene modification method [51]. Briefly, primers with 50 bp of *CDC24* C-terminus and 3'UTR homology were used to amplify the pFA6 3HA *kanMX* cassette. The PCR product was purified and transformed to tag *CDC24* via standard transformation methods. Proper integration was confirmed by PCR and sequencing.

The Bem3-12myc, Rga1-12myc, and Rga2-12myc constructs were made by cloning PCR products encoding the C-termini of the proteins into a pRS306-based integrating plasmid (pSWE1-myc) containing 12 myc tags and the *SWE1* terminator [52]. Digestion at a site within the gene was used to target integration of the plasmid at the endogenous loci, and proper integration was confirmed by PCR checks.

Cells were grown on rich YEPD media (1% yeast extract, 2% peptone, 2% dextrose) or complete synthetic medium (CSM; MP Biomedicals) with 2% dextrose at 24°C as described below.

Isolation and analysis of suppressor mutants

The MATa *gic1Δ gic2Δ* strain DLY20961 was streaked for single colonies on YEPD plates at 24°C. 10 colonies were picked using sterile toothpicks, and the cells were resuspended in 1 mL of sterile distilled water and counted. 1 million cells from each colony were spread onto individual YEPD plates. Each plate was incubated at 37°C for 3 days, after which plates displayed growth of numerous microcolonies and a few large colonies. A large colony was picked from each of the 10 plates, and mated to non-suppressed MATα *gic1Δ gic2Δ* strain DLY21941. Mating was conducted by mixing cells on a YEPD plate, with a large excess of the MATa strain, so that most MATα cells would mate. Cells from the mating mix were spread on YEPD plates containing 2 μ M α -factor to arrest unmated MATa cells, and colonies were tested to determine whether they could sporulate (indicating successful diploid formation) when transferred to 2% Potassium Acetate plates and allowed to grow for 5–7 days.

Asci from sporulating diploids were digested by treatment with lyticase for 5 min. Tetrads were diluted in sterile distilled water, spread on YEPD plates, and dissected with a micromanipulator. Tetrad plates were incubated at 24°C or 37°C as indicated for 3 days. Images of plates were taken on day 3. Spore colonies were replica plated to relevant selective media plates to test for auxotrophic markers. Suppressor strains were then crossed to each other and tetrads were analyzed using a similar procedure.

Cell synchronization

For imaging experiments, the cells were first synchronized by G1 arrest/release. MATa cells were grown overnight at 24°C in CSM+D, adjusted to 1.5×10^7 cells/mL, and treated with 2 μ M α -factor (Genesee Scientific) at 24°C for 3 h. G1-arrested cells were released from arrest by washing two times with fresh medium, and placed on microscope slabs at 37°C for imaging.

Microscopy and image analysis

Cells were mounted on a 250 μ L slab solidified with 2% agarose on a microscope slide. After putting a cover slip on top, the edges were sealed with petroleum jelly to prevent evaporation. Image acquisition was done using an Andor XD Revolution spinning-disk confocal microscope (Olympus) with a Yokogawa CSU-X1 5000 r.p.m. disk unit, and a 100x/1.4 UPlanSApo oil-immersion objective controlled by MetaMorph software (Universal Imaging). The microscope is enclosed in a temperature-controlled chamber that was set to 37°C 1 h prior to imaging. Fluorophores were excited with 488 nm and 561 nm diode lasers. Images (stacks of 17 z planes spaced 0.5 μ m apart) were collected at 1 min intervals using a iXon3 897 EM-CCD camera with 1.2x auxiliary magnification (Andor Technology). Laser power was set to 10% maximum output to reduce phototoxicity. Exposure time was 200 ms for each image. An EM-Gain setting of 200 was used for the EM-CCD camera.

Collected images were deconvolved using Hyugens Essential software (Scientific Volume Imaging). Images were then processed using ImageJ (National Institutes of Health). Z-stacks were collapsed into maximum projection images. Polarization was scored by eye as the first detection of a cluster of the polarity probe (GFP-Cdc42 or Bem1-tdTomato). Whi5 nuclear export was scored using a custom MATLAB graphical user interface (GUI; Nuc-TrackV3.3) as described [53]. This tool allows for designation and tracking of a region of interest at specific times of interest during the course of the time-lapse. For our purposes, regions of interest were individual cells. The coefficient of variation of Whi5 signal intensity between pixels in each cell was measured and used to determine the time point at which 50% of Whi5 exited the nucleus. Calculated values are normalized to peak intensity for each track. This tool is available upon request from Dennis Tsygankov (ude.hcetag.emb@voknagysT.sined).

Immunoblotting

Cells were grown overnight in YEPD at 24°C, and where indicated shifted to 37°C for 6 h prior to harvesting. Cell pellets (about 10^7 cells) were resuspended in 225 μ L cold Pronase buffer (25 mM Tris-HCl, pH 7.5, 1.4 M Sorbitol, 20 mM NaN₃, 2 mM MgCl₂) and 48 μ L of 100% TCA. Pellet-buffer mixture was stored frozen at -80°C. Once thawed on ice, cells were lysed by vortexing with 280 μ L of sterile acid-washed glass beads at 4°C for 10 min. Beads were washed twice with 5% TCA. Lysate was collected and precipitated proteins were pelleted by centrifugation at maximum speed in an Eppendorf centrifuge for 10 min at 4°C. Pellets were solubilized in Thorner buffer (40 mM Tris-HCl, pH 6.8, 8 M Urea, 5% SDS, 143 mM β -mercaptoethanol, 0.1 mM EDTA, 0.4 mg/ml Bromophenol Blue). 2 M Tris base was used to adjust the pH to 8. Samples were heated at 42°C for 3 min prior to loading on a 10% Acrylamide/Bis gel and run for 1 h at 40 mA. Following transfer, membranes were probed with anti-cMyc, or anti-HA (12CA5) (Roche) monoclonal antibodies and anti-Cdc11 polyclonal antibodies (Santa Cruz Biotechnologies) used at 1:1000 and 1:2000 dilution respectively. Secondary antibodies IRDye800-conjugated anti-mouse IgG (Rockland Immunochemicals) and Alexa-fluor680-conjugated goat anti-rabbit IgG (Invitrogen) were used at 1:10,000 dilution. After washing, Western blots were visualized using the ODYSSEY imaging system (Li-COR Biosciences).

Western blot quantification was done using ImageJ to measure band intensity in individual color channels. Mutant and wild-type bands were always compared from the same blot using lanes with comparable Cdc11 loading controls. After dividing by the loading controls, bands were normalized to the wild-type signal.

Supporting information

S1 Movie. Bem1 polarization defect in *gic1 gic2* mutants. Representative cells expressing Whi5-GFP (cell cycle marker) and Bem1-tdTomato (polarity marker). Top: Wildtype (DLY19654). Bottom: *gic1Δ gic2Δ* (DLY20961). Images were acquired at 37°C. Time is in min:s. Scale bar, 5 μm.

(AVI)

S2 Movie. Cdc42 polarization defect in *gic1 gic2* mutants. Representative cells expressing Whi5-tdTomato (cell cycle marker) and GFP-Cdc42 (polarity marker). Top: Wildtype (DLY21726). Bottom: *gic1Δ gic2Δ* (DLY221728). Images were acquired at 37°C. Time is in min:s. Scale bar, 5 μm.

(AVI)

S3 Movie. Restored polarization in suppressed *gic1 gic2* mutants. Representative cells expressing Whi5-GFP (cell cycle marker) and Bem1-tdTomato (polarity marker). Top: Wildtype (DLY19654). Bottom: suppressed *gic1Δ gic2Δ* (DLY22968). Images were acquired at 37°C. Time is in min:s. Scale bar, 5 μm.

(AVI)

S1 Table. Minimal data set. This Table contains the raw data points used to plot the graphs in Figs 2, 3 and 5. Each Fig part is under a separate tab.

(XLSX)

Acknowledgments

We thank Kyle Moran for help with the statistics, and members of the Lew lab for productive discussions and input. This work was funded by NIH/NIGMS grants GM62300 and GM122488 to D.J.L.

Author Contributions

Conceptualization: Christine N. Daniels, Daniel J. Lew.

Funding acquisition: Daniel J. Lew.

Investigation: Christine N. Daniels.

Methodology: Christine N. Daniels, Trevin R. Zyla.

Project administration: Daniel J. Lew.

Resources: Christine N. Daniels, Trevin R. Zyla.

Supervision: Daniel J. Lew.

Writing – original draft: Christine N. Daniels.

Writing – review & editing: Daniel J. Lew.

References

1. Hall A, Paterson HF, Adamson P, Ridley AJ. Cellular responses regulated by rho-related small GTP-binding proteins. [Review]. *Philos Trans R Soc Lond B Biol Sci.* 1993; 340(1293):267–71. <https://doi.org/10.1098/rstb.1993.0067> PMID: 8103928
2. Hodge RG, Ridley AJ. Regulating Rho GTPases and their regulators. *Nat Rev Mol Cell Biol.* 2016; 17(8):496–510. Epub 2016/06/16. <https://doi.org/10.1038/nrm.2016.67> PMID: 27301673.

3. Mitin N, Roberts PJ, Chenette EJ, Der CJ. Posttranslational lipid modification of Rho family small GTPases. *Methods Mol Biol.* 2012; 827:87–95. Epub 2011/12/07. https://doi.org/10.1007/978-1-61779-442-1_6 PMID: 22144269.
4. Boulter E, Garcia-Mata R, Guilluy C, Dubash A, Rossi G, Brenwald PJ, et al. Regulation of Rho GTPase crosstalk, degradation and activity by RhoGDI1. *Nature cell biology.* 2010; 12(5):477–83. Epub 2010/04/20. <https://doi.org/10.1038/ncb2049> PMID: 20400958
5. Rane CK, Minden A. P21 activated kinases: structure, regulation, and functions. *Small Gtpases.* 2014; 5. Epub 2014/03/25. <https://doi.org/10.4161/sgtp.28003> PMID: 24658305
6. Alekhina O, Burstein E, Billadeau DD. Cellular functions of WASP family proteins at a glance. *Journal of cell science.* 2017; 130(14):2235–41. Epub 2017/06/25. <https://doi.org/10.1242/jcs.199570> PMID: 28646090
7. Kovar DR. Molecular details of formin-mediated actin assembly. *Current opinion in cell biology.* 2006; 18(1):11–7. Epub 2005/12/21. <https://doi.org/10.1016/j.ceb.2005.12.011> PMID: 16364624.
8. Etienne-Manneville S. Cdc42—the centre of polarity. *Journal of cell science.* 2004; 117(Pt 8):1291–300. <https://doi.org/10.1242/jcs.01115> PMID: 15020669.
9. Howell AS, Jin M, Wu CF, Zyla TR, Elston TC, Lew DJ. Negative feedback enhances robustness in the yeast polarity establishment circuit. *Cell.* 2012; 149(2):322–33. Epub 2012/04/17. <https://doi.org/10.1016/j.cell.2012.03.012> PMID: 22500799.
10. Chiou JG, Balasubramanian MK, Lew DJ. Cell Polarity in Yeast. *Annu Rev Cell Dev Biol.* 2017; 33:77–101. Epub 2017/08/09. <https://doi.org/10.1146/annurev-cellbio-100616-060856> PMID: 28783960
11. Kozubowski L, Saito K, Johnson JM, Howell AS, Zyla TR, Lew DJ. Symmetry-Breaking Polarization Driven by a Cdc42p GEF-PAK Complex. *Curr Biol.* 2008; 18(22):1719–26. <https://doi.org/10.1016/j.cub.2008.09.060> PMID: 19013066.
12. Johnson JM, Jin M, Lew DJ. Symmetry breaking and the establishment of cell polarity in budding yeast. *Current opinion in genetics & development.* 2011. Epub 2011/10/01. <https://doi.org/10.1016/j.gde.2011.09.007> PMID: 21955794.
13. Gulli MP, Jaquenoud M, Shimada Y, Niederhauser G, Wiget P, Peter M. Phosphorylation of the Cdc42 exchange factor Cdc24 by the PAK-like kinase Cla4 may regulate polarized growth in yeast. *Mol Cell.* 2000; 6:1155–67. PMID: 11106754
14. Bose I, Irazoqui JE, Moskow JJ, Bardes ES, Zyla TR, Lew DJ. Assembly of scaffold-mediated complexes containing Cdc42p, the exchange factor Cdc24p, and the effector Cla4p required for cell cycle-regulated phosphorylation of Cdc24p. *The Journal of biological chemistry.* 2001; 276(10):7176–86. <https://doi.org/10.1074/jbc.M010546200> PMID: 11113154.
15. Wai SC, Gerber SA, Li R. Multisite phosphorylation of the guanine nucleotide exchange factor Cdc24 during yeast cell polarization. *PLoS One.* 2009; 4(8):e6563. Epub 2009/08/12. <https://doi.org/10.1371/journal.pone.0006563> PMID: 19668330
16. Kuo CC, Savage NS, Chen H, Wu CF, Zyla TR, Lew DJ. Inhibitory GEF phosphorylation provides negative feedback in the yeast polarity circuit. *Curr Biol.* 2014; 24(7):753–9. <https://doi.org/10.1016/j.cub.2014.02.024> PMID: 24631237
17. Rapali P, Mitteau R, Braun C, Massoni-Laporte A, Unlu C, Bataille L, et al. Scaffold-mediated gating of Cdc42 signalling flux. *eLife.* 2017; 6. Epub 2017/03/18. <https://doi.org/10.7554/eLife.25257> PMID: 28304276
18. Burbelo PD, Drechsel D, Hall A. A conserved binding motif defines numerous candidate target proteins for both Cdc42 and Rac GTPases. *J Biol Chem.* 1995; 270(49):29071–4. PMID: 7493928
19. Brown JL, Jaquenoud M, Gulli MP, Chant J, Peter M. Novel Cdc42-binding proteins Gic1 and Gic2 control cell polarity in yeast. *Genes Dev.* 1997; 11(22):2972–82. PMID: 9367980
20. Chen GC, Kim YJ, Chan CS. The Cdc42 GTPase-associated proteins Gic1 and Gic2 are required for polarized cell growth in *Saccharomyces cerevisiae*. *Genes Dev.* 1997; 11(22):2958–71. PMID: 9367979
21. Takahashi S, Pryciak PM. Identification of novel membrane-binding domains in multiple yeast Cdc42 effectors. *Molecular biology of the cell.* 2007; 18(12):4945–56. <https://doi.org/10.1091/mbc.E07-07-0676> PMID: 17914055.
22. Jaquenoud M, Peter M. Gic2p may link activated Cdc42p to components involved in actin polarization, including Bni1p and Bud6p (Aip3p). *Molecular and cellular biology.* 2000; 20(17):6244–58. PMID: 10938101
23. Joberty G, Perlungher RR, Macara IG. The Borgs, a new family of Cdc42 and TC10 GTPase-interacting proteins. *Molecular and cellular biology.* 1999; 19(10):6585–97. Epub 1999/09/22. PMID: 10490598

24. Pruyne D, Legesse-Miller A, Gao L, Dong Y, Bretscher A. Mechanisms of polarized growth and organelle segregation in yeast. *Annu Rev Cell Dev Biol.* 2004; 20:559–91. Epub 2004/10/12. <https://doi.org/10.1146/annurev.cellbio.20.010403.103108> PMID: 15473852.
25. Kaksonen M, Toret CP, Drubin DG. Harnessing actin dynamics for clathrin-mediated endocytosis. *Nat Rev Mol Cell Biol.* 2006; 7(6):404–14. <https://doi.org/10.1038/nrm1940> PMID: 16723976.
26. Chen H, Kuo CC, Kang H, Howell AS, Zyla TR, Jin M, et al. Cdc42p regulation of the yeast formin Bni1p mediated by the effector Gic2p. *Molecular biology of the cell.* 2012; 23(19):3814–26. Epub 2012/08/25. <https://doi.org/10.1091/mbc.E12-05-0400> PMID: 22918946
27. Gladfelter AS, Pringle JR, Lew DJ. The septin cortex at the yeast mother-bud neck. *Curr Opin Microbiol.* 2001; 4:681–9. PMID: 11731320
28. Oh Y, Bi E. Septin structure and function in yeast and beyond. *Trends Cell Biol.* 2011; 21(3):141–8. Epub 2010/12/24. <https://doi.org/10.1016/j.tcb.2010.11.006> PMID: 21177106
29. Iwase M, Luo J, Nagaraj S, Longtine M, Kim HB, Haarer BK, et al. Role of a Cdc42p effector pathway in recruitment of the yeast septins to the presumptive bud site. *Molecular biology of the cell.* 2006; 17(3):1110–25. <https://doi.org/10.1091/mbc.E05-08-0793> PMID: 16371506.
30. Sadian Y, Gatsogiannis C, Patasi C, Hofnagel O, Goody RS, Farkasovsky M, et al. The role of Cdc42 and Gic1 in the regulation of septin filament formation and dissociation. *eLife.* 2013; 2:e01085. Epub 2013/11/30. <https://doi.org/10.7554/eLife.01085> PMID: 24286829
31. Kawasaki R, Fujimura-Kamada K, Toi H, Kato H, Tanaka K. The upstream regulator, Rsr1p, and downstream effectors, Gic1p and Gic2p, of the Cdc42p small GTPase coordinately regulate initiation of budding in *Saccharomyces cerevisiae*. *Genes Cells.* 2003; 8(3):235–50. PMID: 12622721.
32. Howell AS, Lew DJ. Morphogenesis and the cell cycle. *Genetics.* 2012; 190(1):51–77. Epub 2012/01/06. <https://doi.org/10.1534/genetics.111.128314> PMID: 22219508
33. Costanzo M, Nishikawa JL, Tang X, Millman JS, Schub O, Breitzkreuz K, et al. CDK activity antagonizes Whi5, an inhibitor of G1/S transcription in yeast. *Cell.* 2004; 117(7):899–913. <https://doi.org/10.1016/j.cell.2004.05.024> PMID: 15210111.
34. de Bruin RA, McDonald WH, Kalashnikova TI, Yates J 3rd, Wittenberg C. Cln3 activates G1-specific transcription via phosphorylation of the SBF bound repressor Whi5. *Cell.* 2004; 117(7):887–98. <https://doi.org/10.1016/j.cell.2004.05.025> PMID: 15210110.
35. Skotheim JM, Di Talia S, Siggia ED, Cross FR. Positive feedback of G1 cyclins ensures coherent cell cycle entry. *Nature.* 2008; 454(7202):291–6. <https://doi.org/10.1038/nature07118> PMID: 18633409.
36. Doncic A, Falleur-Fettig M, Skotheim JM. Distinct interactions select and maintain a specific cell fate. *Molecular cell.* 2011; 43(4):528–39. Epub 2011/08/23. <https://doi.org/10.1016/j.molcel.2011.06.025> PMID: 21855793
37. Knaus M, Pelli-Gulli MP, van Drogen F, Springer S, Jaquenoud M, Peter M. Phosphorylation of Bem2p and Bem3p may contribute to local activation of Cdc42p at bud emergence. *The EMBO journal.* 2007; 26(21):4501–13. <https://doi.org/10.1038/sj.emboj.7601873> PMID: 17914457.
38. Sopko R, Huang D, Smith JC, Figeys D, Andrews BJ. Activation of the Cdc42p GTPase by cyclin-dependent protein kinases in budding yeast. *The EMBO journal.* 2007; 26(21):4487–500. <https://doi.org/10.1038/sj.emboj.7601847> PMID: 17853895.
39. Ayscough KR, Stryker J, Pokala N, Sanders M, Crews P, Drubin DG. High rates of actin filament turnover in budding yeast and roles for actin in establishment and maintenance of cell polarity revealed using the actin inhibitor latrunculin-A. *J Cell Biol.* 1997; 137:399–416. PMID: 9128251
40. Irazoqui JE, Gladfelter AS, Lew DJ. Scaffold-mediated symmetry breaking by Cdc42p. *Nature cell biology.* 2003; 5(12):1062–70. <https://doi.org/10.1038/ncb1068> PMID: 14625559.
41. Pringle JR, Bi E, Harkins HA, Zahner JE, De Virgilio C, Chant J, et al. Establishment of cell polarity in yeast. *Cold Spring Harbor Symp Quant Biol.* 1995; 60:729–44. PMID: 8824448
42. Delley PA, Hall MN. Cell wall stress depolarizes cell growth via hyperactivation of RHO1. *J Cell Biol.* 1999; 147(1):163–74. PMID: 10508863
43. Mutavchiev DR, Leda M, Sawin KE. Remodeling of the Fission Yeast Cdc42 Cell-Polarity Module via the Sty1 p38 Stress-Activated Protein Kinase Pathway. *Curr Biol.* 2016; 26(21):2921–8. <https://doi.org/10.1016/j.cub.2016.08.048> PMID: 27746023
44. Bi E, Chiavetta JB, Chen H, Chen GC, Chan CS, Pringle JR. Identification of novel, evolutionarily conserved Cdc42p-interacting proteins and of redundant pathways linking Cdc24p and Cdc42p to actin polarization in yeast. *Molecular biology of the cell.* 2000; 11(2):773–93. <https://doi.org/10.1091/mbc.11.2.773> PMID: 10679030
45. Kang PJ, Miller KE, Guegueniat J, Beven L, Park HO. The shared role of the Rsr1 GTPase and Gic1/Gic2 in Cdc42 polarization. *Molecular biology of the cell.* 2018; 29(20):2359–69. Epub 2018/08/10. <https://doi.org/10.1091/mbc.E18-02-0145> PMID: 30091649.

46. Bi E, Pringle JR. *ZDS1* and *ZDS2*, genes whose products may regulate Cdc42p in *Saccharomyces cerevisiae*. *Mol Cell Biol*. 1996; 16(10):5264–75. PMID: [8816439](#)
47. Baudin A, Ozier-Kalogeropoulos O, Denouel A, Lacroute F, Cullin C. A simple and efficient method for direct gene deletion in *Saccharomyces cerevisiae*. *Nucleic Acids Res*. 1993; 21(14):3329–30. PMID: [8341614](#)
48. Boeke JD, Trueheart J, Natsoulis G, Fink GR. 5-Fluoroorotic acid as a selective agent in yeast molecular genetics. *Meth Enzymol*. 1987; 154:164–73. PMID: [3323810](#)
49. Liu X, Wang X, Yang X, Liu S, Jiang L, Qu Y, et al. Reliable cell cycle commitment in budding yeast is ensured by signal integration. *eLife*. 2015; 4. Epub 2015/01/16. <https://doi.org/10.7554/eLife.03977> PMID: [25590650](#)
50. Marquitz AR, Harrison JC, Bose I, Zyla TR, McMillan JN, Lew DJ. The Rho-GAP Bem2p plays a GAP-independent role in the morphogenesis checkpoint. *The EMBO journal*. 2002; 21(15):4012–25. <https://doi.org/10.1093/emboj/cdf416> PMID: [12145202](#).
51. Longtine MS, McKenzie A III, DeMarini DJ, Shah NG, Wach A, Brachat A, et al. Additional modules for versatile and economical PCR-based gene deletion and modification in *Saccharomyces cerevisiae*. *Yeast (Chichester, England)*. 1998; 14(10):953–61.
52. McMillan JN, Sia RAL, Lew DJ. A morphogenesis checkpoint monitors the actin cytoskeleton in yeast. *J Cell Biol*. 1998; 142:1487–99. PMID: [9744879](#)
53. Simons JF, Ferro-Novick S, Rose MD, Helenius A. BiP/Kar2p serves as a molecular chaperone during carboxypeptidase Y folding in yeast. *The Journal of cell biology*. 1995; 130(1):41–9. PMID: [7790376](#)